UNIVERSITAT POLITÈCNICA
DE CATALUNYA
BARCELONATECH

CIMNE

CIMNE Coffee Talk

Simulating viscoelastic fluid flows with high Weissenberg number

Laura Moreno Martínez
Advisors: Ramon Codina and Joan Baiges

December, 2019

Outline

Introduction: What is viscoelasticity?

- Fluids depending on their behaviour under **the action of shear stress**, can be classified as Newtonian and non-Newtonian
- Viscoelastic fluids are a specific type of **non-Newtonian fluids** that exhibits a combination of elastic and viscous effects.
    - **Visco**: friction, irreversibility, loss of memory.
    - **Elastic**: recoil, internal energy storage.
- They have "**memory**": the state-of-stress depends on the flow history.

Introduction: Heat transfer processes

- Viscoelastic fluids have very **advantageous properties** for heat transfer and transport:
- As the Weissenberg number increases, the dynamics of viscoelastic fluid change. This turn out in a **higher mixing capacity**, with benefits in the heat transfer between the fluid and the pipe transporting it.

- **Examples**: Fire brigades water tanks, petroleum extraction, reducing the drag forces in submarines, chemical reactors.


Introduction: Modelling of polymeric fluids

Deviatoric extra stress tensor

- Momentum equation:

$$\rho\frac{\partial \boldsymbol{u}}{\partial t} + \rho\boldsymbol{u}\cdot\nabla\boldsymbol{u} - \nabla\cdot\mathbf{T} + \nabla p = \boldsymbol{f}$$

$$\boxed{\mathbf{T} = 2\eta(\nabla^s\boldsymbol{u})}$$

Newtonian viscous fluids

- Continuity equation:

$$\nabla\cdot\boldsymbol{u} = 0$$

$$\boxed{\mathbf{T} = 2\eta_s(\nabla^s\boldsymbol{u}) + \boldsymbol{\sigma}}$$

Polymeric fluids

- Constitutive equation:

$$\frac{1}{2\eta_p}(1 + h(\boldsymbol{\sigma}))\cdot\boldsymbol{\sigma} - \nabla^s\boldsymbol{u} + \frac{\lambda}{2\eta_p}\left(\frac{\partial\boldsymbol{\sigma}}{\partial t} + \boldsymbol{u}\cdot\nabla\boldsymbol{\sigma} - \boldsymbol{\sigma}\cdot\nabla\boldsymbol{u} + (\nabla\boldsymbol{u}^T)\cdot\boldsymbol{\sigma}\right) = \mathbf{0}$$

$$\boxed{h(\boldsymbol{\sigma}) = 0}$$

Oldroyd-B

$$\boxed{h(\boldsymbol{\sigma}) = \frac{\epsilon\lambda}{\eta_p}\boldsymbol{\sigma}}$$

Giesekus

$$\boxed{h(\boldsymbol{\sigma}) = \frac{\epsilon\lambda}{\eta_p}\mathrm{tr}(\boldsymbol{\sigma})}$$

Phan-Thien-Tanner

Introduction: The Weissenberg number

$$\boxed{\lambda \text{ : Relaxation time}}$$

$$\frac{1}{2\eta_p}(1+h(\boldsymbol{\sigma}))\cdot\boldsymbol{\sigma} - \nabla^s \boldsymbol{u} + \frac{\lambda}{2\eta_p}\left(\frac{\partial\boldsymbol{\sigma}}{\partial t} + \overbrace{\boldsymbol{u}\cdot\nabla\boldsymbol{\sigma}}^{\text{convective term}} \overbrace{-\boldsymbol{\sigma}\cdot\nabla\boldsymbol{u} + (\nabla\boldsymbol{u}^T)\cdot\boldsymbol{\sigma}}^{\text{deformation terms}}\right) = \mathbf{0}$$

- We is small: Newtonian viscosity fluid.
- When We > 1: problems are extremally complicated.

$$\boxed{\mathrm{We} = \lambda\frac{U}{L}}$$

The High Weissenberg Number Problem

1. Computational rheology: **1970s**. FEM steady 2D flows.
2. All methods, were found to **breakdown** at a low Weissenberg number.
3. The breakdown occurs for a **critical value** of the Weissenberg number, but it is specific to each problem.
4. For approximately 30 years, the reason for this breakdown has been a **mystery**, although it had been associated to a *numerical phenomenon*.

Logarithmic conformation formulation

Main features

- Proposed by **Fattal and Kupferman** (2004).
- Treats the **exponential growth** of the elastic stresses when the elastic component becomes dominant.
- Allows to **extend the range** of Weissenberg numbers. ✓
- More computational **expensive** than the standard formulation. ✗

- Physically-admissible conformation tensors must be **symmetric** and **positive-definite**.

Elastic stress tensor

$$\boldsymbol{\sigma} = \frac{\eta_p}{\lambda}(\boldsymbol{\tau} - \mathbf{I}) \longrightarrow \boldsymbol{\tau} = \frac{\lambda \boldsymbol{\sigma}}{\eta_p} + \mathbf{I}$$

Conformation tensor

- Conformation tensor is replaced by $\boxed{\psi = \log(\boldsymbol{\tau}).}$

New set of equations

$$\boxed{\psi = \log(\frac{\lambda_0 \boldsymbol{\sigma}}{\eta_p} + \mathbf{I}) \longrightarrow \boldsymbol{\sigma} = \frac{\eta_p}{\lambda_0}(\exp(\psi) - \mathbf{I})}$$

Change of variable employed

$$\boxed{\lambda_0 = \max\{k\lambda, \lambda_{0,\min}\}}$$

- Momentum equation:

$$-\frac{\eta_p}{\lambda_0}\nabla \cdot \exp(\psi) - 2\eta_e \nabla \cdot (\nabla^s \boldsymbol{u}) + \rho \boldsymbol{u} \cdot \nabla \boldsymbol{u} + \nabla p = \boldsymbol{f}$$

- Continuity equation:

$$\nabla \cdot \boldsymbol{u} = 0$$

New non-linearities!!

- Constitutive equation:

$$\frac{1}{2\lambda_0}(\exp(\psi) - \mathbf{I}) - \nabla^s \boldsymbol{u} + \frac{\lambda}{2\lambda_0}\left(\boldsymbol{u} \cdot \nabla \exp\left(\psi\right)\right)$$
$$+ \frac{\lambda}{2\lambda_0}\left(-\exp\left(\psi\right) \cdot \nabla \boldsymbol{u} - \left(\nabla \boldsymbol{u}\right)^T \cdot \exp\left(\psi\right) + 2\nabla^s \boldsymbol{u}\right) = \mathbf{0}$$

Linearization of the exponential

$$\exp(\boldsymbol{\psi}) = \underbrace{\exp(\hat{\boldsymbol{\psi}} + \delta\boldsymbol{\psi})} = \exp(\hat{\boldsymbol{\psi}}) \cdot \underbrace{\exp(\delta\boldsymbol{\psi})}$$

$$\boxed{\exp(\delta\boldsymbol{\psi}) \approx \boldsymbol{I} + \delta\boldsymbol{\psi}}$$

Taylor expansion

- $\delta\boldsymbol{\psi} = \boldsymbol{\psi} - \hat{\boldsymbol{\psi}}$ is the incremental part
- $\hat{\boldsymbol{\psi}}$ is a known tensor, calculated at the previous iteration

Consequently,

$$\exp(\boldsymbol{\psi}) \approx \exp(\hat{\boldsymbol{\psi}}) \cdot (\boldsymbol{I} + \delta\boldsymbol{\psi}) = \exp(\hat{\boldsymbol{\psi}}) \cdot \boldsymbol{\psi} + \exp(\hat{\boldsymbol{\psi}}) \cdot (\boldsymbol{I} - \hat{\boldsymbol{\psi}}).$$

Spatial and temporal discretization

- **Galerkin FE** approximation. Consists in finding $\boldsymbol{U}_h : (0, t_{\mathrm{f}}) \longrightarrow \boldsymbol{\mathcal{X}}_h$,

$$\underbrace{(\mathcal{D}_t(\boldsymbol{U}_h), \boldsymbol{V}_h)}_{\text{Temporal terms}} + \underbrace{B(\boldsymbol{u}_{;}\boldsymbol{U}_h, \boldsymbol{V}_h)}_{\text{Bilinear form}} = L(\boldsymbol{V}_h),$$

  for all $\boldsymbol{V}_h = [\boldsymbol{v}_h, q_h, \chi_h] \in \boldsymbol{\mathcal{X}}_h$

- Monolithic **time discretization** the simplest BDF1 scheme

$$\frac{\delta_1 f^{n+1}}{\delta t} = \frac{f^{n+1} - f^n}{\delta t} = \left.\frac{\partial f}{\partial t}\right|_{t^{n+1}} + \mathcal{O}(\delta t).$$

$$\left.\frac{\partial(\exp(\psi))}{\partial t}\right|_{t^{n+1}} = \frac{1}{\delta t}\Big[\exp(\hat{\psi}^{n+1}) \cdot \psi^{n+1} + \exp(\hat{\psi}^{n+1}) - \exp(\hat{\psi}^{n+1}) \cdot \hat{\psi}^{n+1}$$
$$- \exp(\psi^n)\Big] + \mathcal{O}(\delta t) + \mathcal{O}((\delta \psi^{n+1})^2).$$

Stabilized formulation: Variational multiscale methods

- To approximate the components of the continuous problem solution that cannot be resolved by the finite element mesh.
- Split the unknowns as $\boldsymbol{U} = \underbrace{\boldsymbol{U}_h}_{\in \boldsymbol{\mathcal{X}_h}} + \underbrace{\tilde{\boldsymbol{U}}}_{\in \tilde{\boldsymbol{\mathcal{X}}}}$ and $\boldsymbol{\mathcal{X}} = \boldsymbol{\mathcal{X}_h} \bigoplus \tilde{\boldsymbol{\mathcal{X}}}$.

$$\boxed{\tilde{\boldsymbol{U}} = \boldsymbol{\alpha} \tilde{P}[\mathbf{F} - \mathcal{D}_t(\boldsymbol{U}_h) - \mathcal{L}(\boldsymbol{u}_h; \boldsymbol{U}_h)]}$$

Sub-grid scale

$$\underbrace{\underbrace{(\mathcal{D}_t(\boldsymbol{U}_h), \boldsymbol{V}_h)}_{\text{Temporal terms}} + \underbrace{B(\boldsymbol{u}_h; \boldsymbol{U}_h, \boldsymbol{V}_h)}_{\text{Bilinear terms}}}_{\text{Galerkin terms}} + \underbrace{\sum_K \langle \tilde{\boldsymbol{U}}, \underbrace{\mathcal{L}^*(\boldsymbol{u}_h; \boldsymbol{V}_h)}_{\text{adjoint operator of } \mathcal{L}} \rangle_K}_{\text{Stabilization terms}} = L(\boldsymbol{V}_h)$$

- $\tilde{P}$ is the L^2 projection onto the space of sub-grid scales,
- $\boldsymbol{\alpha}$ is a matrix computed within each element,
- $\mathcal{L}$ is the operator associated to the problem.

Stabilized formulation: Main operators

$$\boxed{\overbrace{(\mathcal{D}_t(\boldsymbol{U}_h),\boldsymbol{V}_h)+B(\boldsymbol{u}_h;\boldsymbol{U}_h,\boldsymbol{V}_h)}^{\text{Galerkin terms}}+\overbrace{\sum_K\langle\underbrace{\boldsymbol{\alpha}\tilde{P}[\mathbf{F}-\mathcal{D}_t(\boldsymbol{U}_h)-\mathcal{L}(\boldsymbol{u}_h;\boldsymbol{U}_h)]}_{\tilde{\boldsymbol{U}}},\mathcal{L}_0^*(\boldsymbol{u}_h;\boldsymbol{V}_h)\rangle_K}^{\text{Stabilization terms}}=L(\boldsymbol{V}_h)}$$

$$\mathcal{L}(\hat{\boldsymbol{u}};\boldsymbol{U}):=\begin{pmatrix} -\dfrac{\eta_p}{\lambda_0}\nabla\cdot(\exp(\boldsymbol{\psi}))-2\eta_e\nabla\cdot(\nabla^s\boldsymbol{u})+\rho\hat{\boldsymbol{u}}\cdot\nabla\boldsymbol{u}+\nabla p \\ \nabla\cdot\boldsymbol{u} \\ \dfrac{1}{2\lambda_0}\exp(\boldsymbol{\psi})-\nabla^s\boldsymbol{u}+\dfrac{\lambda}{2\lambda_0}(\hat{\boldsymbol{u}}\cdot\nabla(\exp(\boldsymbol{\psi})) \\ -\exp(\boldsymbol{\psi})\cdot\nabla\hat{\boldsymbol{u}}-(\nabla\hat{\boldsymbol{u}})^T\cdot\exp(\boldsymbol{\psi})+2\nabla^s\boldsymbol{u}\Big) \end{pmatrix}\begin{array}{l}\longleftarrow\text{Momentum}\\ \longleftarrow\text{Continuity}\\ \longleftarrow\text{Constitutive}\end{array}$$

$$\mathcal{L}_0^*(\hat{\boldsymbol{u}};\boldsymbol{V}):=\begin{pmatrix} \nabla\cdot\boldsymbol{\chi}-2\eta_e\nabla\cdot(\nabla^s\boldsymbol{v})-\rho\hat{\boldsymbol{u}}\cdot\nabla\boldsymbol{v}-\nabla q \\ -\nabla\cdot\boldsymbol{v} \\ \dfrac{1}{2\eta_p}\boldsymbol{\chi}+\nabla^s\boldsymbol{v}-\dfrac{\lambda}{2\eta_p}\left(\hat{\boldsymbol{u}}\cdot\nabla\boldsymbol{\chi}+\boldsymbol{\chi}\cdot(\nabla\hat{\boldsymbol{u}})^T+\nabla\hat{\boldsymbol{u}}\cdot\boldsymbol{\chi}\right) \end{pmatrix}$$

Stabilized formulation: Residual based vs Split OSS

$$\underbrace{\mathcal{D}_t(\boldsymbol{U}_h), \boldsymbol{V}_h) + B(\boldsymbol{u}_h; \boldsymbol{U}_h, \boldsymbol{V}_h)}_{\text{Galerkin terms}} + \overbrace{S_1(\boldsymbol{u}_h; \boldsymbol{U}_h, \boldsymbol{V}_h) + S_2(\boldsymbol{U}_h, \boldsymbol{V}_h) + S_3(\boldsymbol{u}_h; \boldsymbol{U}_h, \boldsymbol{V}_h)}^{\text{Stabilization terms}} = \underbrace{L(\boldsymbol{V}_h)}_{\text{Gal. term}} + \overbrace{R_1(\boldsymbol{u}_h) + R_3(\boldsymbol{u}_h)}^{\text{Stab. term}}$$

$$S_1(\hat{\boldsymbol{u}}_h; \boldsymbol{U}_h, \boldsymbol{V}_h) = \sum_K \alpha_1 \Big\langle \tilde{P}\Big[\rho \frac{\partial \boldsymbol{u}_h}{\partial t} - \frac{\eta_p}{\lambda_0} \nabla \cdot (\exp(\boldsymbol{\psi}_h)) - 2\eta_e \nabla \cdot (\nabla^s \boldsymbol{u}_h) + \rho \hat{\boldsymbol{u}}_h \cdot \nabla \boldsymbol{u}_h + \nabla p_h\Big],$$
$$-\nabla \cdot \boldsymbol{\chi}_h + 2\eta_e \nabla \cdot (\nabla^s \boldsymbol{v}_h) + \rho \hat{\boldsymbol{u}}_h \cdot \nabla \boldsymbol{v}_h + \nabla q_h \Big\rangle_K$$

$$\boxed{\tilde{P} = P_h^{\perp}}$$

Split OSS

1. The **residual** based stabilization contemplates all terms.
2. **Split** OSS stabilization: neglect the cross local inner-product terms as well as some other terms that do not contribute to stability.

Stabilized formulation: Some remarks

Benefits of Split vs Residual stabilization

- **Simpler** than the residual. ✓
- For smooth solutions, it presents **optimal convergence**. ✓
- More **robust** if the solutions has strong gradients. ✓

Remarks: Linearized problem and algorithm

- Non-linear terms are linearized with the **Newton-Raphson's method**.
- Tensors $\hat{\psi}$ and $\hat{\boldsymbol{u}}$ are obtained from the **previous iteration** of the current time step.
- The **orthogonal projection** of any function **f** has been approximated as $P_h^{\perp}(f^i) \approx f^i - P_h(f^{i-1})$.

Validation: Flow over a cylinder

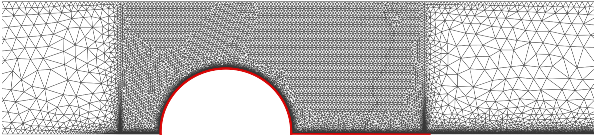

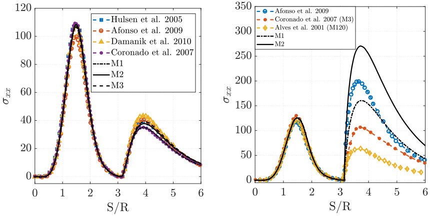

We = 0.7

We = 0.9

Profile of the first component stress (σ_{xx}) along a cylinder and downstream.

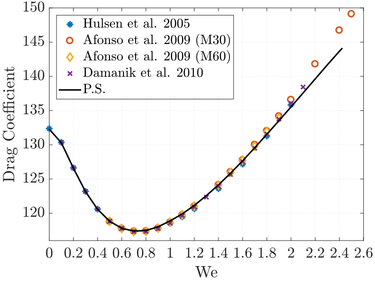

Comparison of drag force coefficient.

Standard formulation break down around We=0.9. The logarithmic formulation **shows good stability for higher values.**

Validation: Contraction 4:1

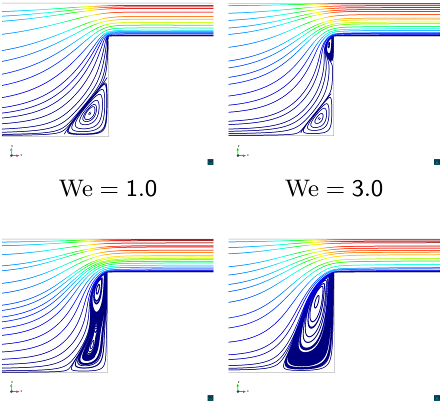

$\mathrm{We} = 1.0$ $\mathrm{We} = 3.0$

$\mathrm{We} = 5.0$ $\mathrm{We} = 7.0$

Streamlines patterns in the contraction planar for different Weissenberg number and $\mathrm{Re} = 0.01$.

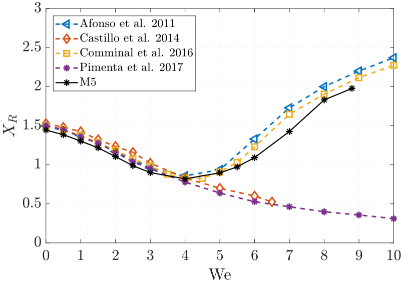

Corner vortex length comparison with finer mesh.

- Standard form. is able to simulate **until We=6.5** approx.
- Logarithmic formulation **until We=15** with the coarsest mesh.

Dynamic Subscales: Why are these necessary?

Classical residual-based stabilized methods for unsteady incompressible flows may experience **difficulties when the time step is small** relative to the spatial grid size.

- Bochev et al. argue that $\delta t > Ch^2$ **a sufficient condition** to avoid instabilities.
- For anisotropic space-time discretizations, this inequality **is not necessarily satisfied**: a very common issue in viscoelastic flow formulations.

Consequently...

New stabilization techniques must be designed to compute time-dependent viscoelastic flow problems with high elasticity and anisotropic space-time discretization.

Dynamic subscales: Adding a temporal derivative

$$\underbrace{\underbrace{(\mathcal{D}_t(\boldsymbol{U}_h), \boldsymbol{V}_h)}_{\text{Temporal terms}} + \underbrace{B(\boldsymbol{u}_h; \boldsymbol{U}_h, \boldsymbol{V}_h)}_{\text{Bilinear terms}}}_{\text{Galerkin terms}} + \underbrace{\sum_K \langle \tilde{\boldsymbol{U}}, \underbrace{\mathcal{L}^*(\boldsymbol{u}_h; \boldsymbol{V}_h)}_{\text{adjoint operator of } \mathcal{L}} \rangle_K}_{\text{Stabilization terms}} = L(\boldsymbol{V}_h)$$

- Quasi-static subscales:

$$\boldsymbol{\alpha}^{-1}\tilde{\boldsymbol{U}} = \tilde{P}[\boldsymbol{F} - \mathcal{D}_t(\boldsymbol{U}_h) - \mathcal{L}(\boldsymbol{u}_h; \boldsymbol{U}_h)]$$

- Dynamic subscales:

$$\boxed{\frac{\partial \tilde{\boldsymbol{U}}}{\partial t} + \boldsymbol{\alpha}^{-1}\tilde{\boldsymbol{U}} = \tilde{P}[\boldsymbol{F} - \mathcal{D}_t(\boldsymbol{U}_h) - \mathcal{L}(\boldsymbol{u}_h; \boldsymbol{U}_h)]}$$

Dynamic subscales for residual-base stabilized formulation

$$\underbrace{\mathcal{D}_t(\boldsymbol{U}_h), \boldsymbol{V}_h) + B(\boldsymbol{u}_h; \boldsymbol{U}_h, \boldsymbol{V}_h)}_{\text{Galerkin terms}} + \overbrace{S_1(\boldsymbol{u}_h; \boldsymbol{U}_h, \boldsymbol{V}_h) + S_2(\boldsymbol{U}_h, \boldsymbol{V}_h) + S_3(\boldsymbol{u}_h; \boldsymbol{U}_h, \boldsymbol{V}_h)}^{\textbf{Stabilization terms}} = \underbrace{L(\boldsymbol{V}_h)}_{\text{Gal. term}} + \overbrace{R_1(\boldsymbol{u}_h) + R_3(\boldsymbol{u}_h)}^{\textbf{Stab. term}}$$

$$S_1(\hat{\boldsymbol{u}}_h; \boldsymbol{U}_h, \boldsymbol{V}_h) = \sum_K \left\langle \tilde{\boldsymbol{u}}, -\nabla \cdot \chi_h + 2\beta\eta_0 \nabla \cdot (\nabla^s \boldsymbol{v}_h) + \rho \hat{\boldsymbol{u}}_h \cdot \nabla \boldsymbol{v}_h + \nabla q_h \right\rangle_K$$

$$\rho \frac{\partial \tilde{\boldsymbol{u}}}{\partial t} + \alpha_1^{-1} \tilde{\boldsymbol{u}} = \tilde{P}\overbrace{(\boldsymbol{F}_1 - \rho \frac{\partial \boldsymbol{u}_h}{\partial t} - \mathcal{L}_1(\boldsymbol{u}_h; \boldsymbol{U}_h))}^{\text{Momentum eq. residual}},$$

$$\boxed{\tilde{\boldsymbol{u}}_1^{n+1} = \underbrace{\left(\rho \frac{1}{\delta t} + \frac{1}{\alpha_1^{n+1}}\right)^{-1}}_{\alpha_{1\text{dyn}}} \left(\rho \frac{1}{\delta t} \tilde{\boldsymbol{u}}_1^n - \rho \tilde{P}(\boldsymbol{F}_1 - \rho \frac{\partial \boldsymbol{u}_h}{\partial t} - \mathcal{L}_1(\boldsymbol{u}_h; \boldsymbol{U}_h))\right)}$$

Discretization using a BDF1 scheme

Dynamic subscales for the term-by-term stabilized formulation (SOSS)

$$S_1(\hat{\boldsymbol{u}}_h; \boldsymbol{U}_h, \boldsymbol{V}_h) = \boxed{\sum_K \langle \tilde{\boldsymbol{u}}_1, -\rho \boldsymbol{u}_h \cdot \nabla \boldsymbol{v}_h \rangle_K} + \sum_K \langle \tilde{\boldsymbol{u}}_2, -\nabla q_h \rangle_K$$

$$+ \sum_K \langle \tilde{\boldsymbol{u}}_3, \nabla \cdot \boldsymbol{\chi}_h \rangle_K + \sum_K \langle \tilde{p}, -\nabla \cdot \boldsymbol{v}_h \rangle_K$$

$$\rho \frac{\partial \tilde{\boldsymbol{u}}_1}{\partial t} + \alpha_1^{-1} \tilde{\boldsymbol{u}}_1 = -P_h^{\perp}(\rho \boldsymbol{u}_h \cdot \nabla \boldsymbol{u}_h),$$

$$\boxed{\tilde{\boldsymbol{u}}_1^{n+1} = \underbrace{\left(\rho \frac{1}{\delta t} + \frac{1}{\alpha_1^{n+1}}\right)^{-1}}_{\alpha_{1\mathrm{dyn}}} \left(\rho \frac{1}{\delta t} \tilde{\boldsymbol{u}}_1^{n} - \rho P_h^{\perp}(\boldsymbol{u}_h^{n+1} \cdot \nabla \boldsymbol{u}_h^{n+1})\right)}$$

Example: Flow over a cylinder. Comparing stabilizations

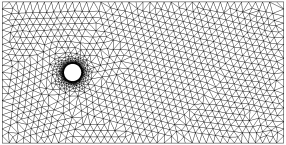

Coarse mesh

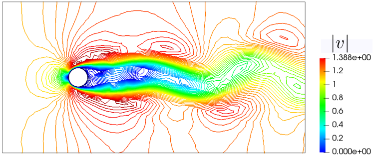

$\delta t = 0.1$

P1 elements	**Time step (δt)**			
Method	0.050	0.0250	3.125×10^{-3}	1.562×10^{-3}
Static-OSS	Solved	Failed	-	-
Dyn-OSS	Solved	Solved	Solved	Solved
Static-SOSS	Solved	Solved	Solved	Failed
Dyn-SOSS	Solved	Solved	Solved	Solved

Table: Solved and failed cases $\mathrm{We} = 0.125$, $\alpha_{1,\mathrm{min}} \approx 1.156 \times 10^{-3}$.

The most unstable stabilization is the **quasi-static** + OSS stabilization.

Example: Flow over a cylinder. Comparing formulations

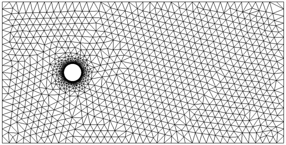

Coarse mesh

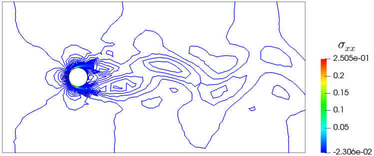

$\delta t = 0.1$

	Weissenberg (We)			
Formulation	0.125	0.165	0.25	0.5
Std-Static	Solved	Failed	-	-
Std-Dyn	Solved	Solved	Solved	Failed
Log-Static	Solved	Solved	Failed	-
Log-Dyn	Solved	Solved	Solved	Solved

Table: Solved and failed cases for S-OSS formulations, dynamic and quasi-static, $\delta t = 0.1$.

Dynamic formulations are more efficient avoiding elastic instabilities.

Benchmark: Lid-driven cavity flow problem

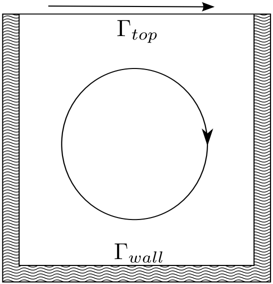

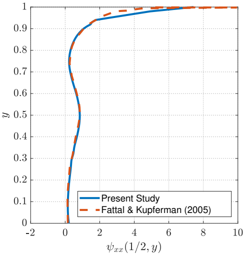

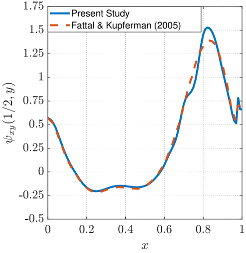

	Stabilization S-OSS	
Formulation	Quasi-static	Dynamic
Standard	Failed - time step 265	Failed - time step 1316
Logarithmic	Failed - time step 340	Solved

Table: Comparison between different formulations, $\mathrm{We} = 1.0$, $\delta t = 0.0025$. The time step at which convergence fails is indicated.

Thermal coupling

- **Energy equation** is added:

$$\boxed{\rho C_p \left(\frac{\partial \theta}{\partial t} + \mathbf{u} \cdot \nabla \theta \right) = k \Delta \theta + \underbrace{\boldsymbol{\sigma} : \nabla^s \mathbf{u}}_{\text{Viscous dissipation}}}$$

- **Viscosity and relaxation time** parameters now will be temperature dependent: $\lambda(\theta) = \lambda(\theta_0) f(\theta)$, and $\eta_0(\theta) = \eta_0(\theta_0) f(\theta)$

$$\boxed{f(\theta) = \exp\left[- \frac{c_1 \cdot (\theta - \theta_0)}{c_2 + (\theta - \theta_0)} \right]}$$

WLF model

$$\boxed{f(\theta) = \exp\left[\alpha \left(\frac{1}{\theta} - \frac{1}{\theta_0} \right) \right]}$$

Arrhenius model

- **Algorithm**: iterative, non-monolithic, executed in a partitioned manner

Validation: Flow around a cylinder

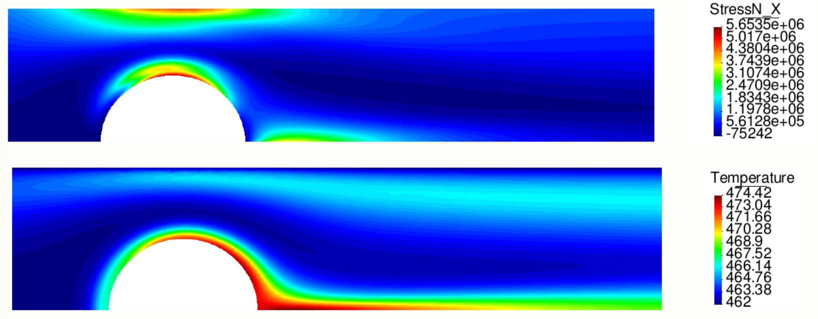

- Distribution of temperature (K) (below) and stress component (top) around the cylinder for We=4.
- Temperature **rise** as function of the Weissenberg number.
- **Reduction of the stress** when temperature increase, due to the heating of the material.

Validation: Extension 1:3

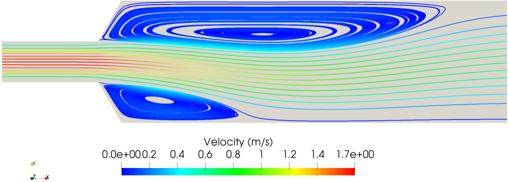

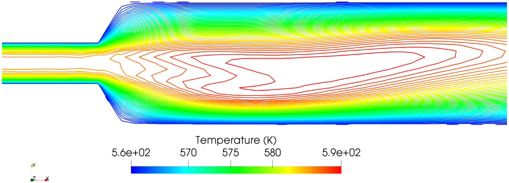

Temperature on the walls (563 K) is greater than the fluid temperature at the inlet (463 K).

However, **viscous dissipation** generates thermal energy in the flowing fluid.

Highest temperature is reached in the **central zone**.

Conclusions

1. The convergence of the proposed method has a strong dependency on the treatment of the **exponential function**.
2. The resulting method allows to obtain **globally stable solutions**, validated in different benchmarks.
3. It shows **accuracy**, optimal convergence for smooth solutions and robustness.
4. **Dynamic subscales** allow to solve problems where two different sources of instability can appear simultaneouly: one originated by a time step small and the other the exponential growth typical of high Weissenberg numbers.
5. In thermal coupling the **viscous dissipation effect** is significant, especially for high-velocity flows or highly viscous flows even at moderate velocities.

References

Presentation based on the next papers:

- L.Moreno, R. Codina, J.Baiges and E. Castillo. Logarithmic conformation reformulation in viscoelastic flow problems approximated by a VMS-type stabilized finite element formulation. Computer Methods in Applied Mechanics and Engineering. 2019 Sep 1;354:706-31
- L. Moreno, R. Codina and J.Baiges. Solution of transient viscoelastic flow problems aproximated by a term-by-term VMS stabilized finite element formulation using time-dependent subgrid-scales.

References

- R. Fattal and R. Kupferman. Constitutive laws for the matrix-logarithm of the conformation tensor. Journal of Non-Newtonian Fluid Mechanics, 123(2-3):281–285, 2004.
- Variational multi-scale stabilized formulations for the stationary three-field incompressible viscoelastic flow problem. Computer Methods in Applied Mechanics and Engineering, 279:579–605, 2014.
- M. A Hulsen, R. Fattal, and R. Kupferman. Flow of viscoelastic fluids past a cylinder at high weissenberg number: stabilized simulations using matrix logarithms. Journal of Non-Newtonian Fluid Mechanics, 127(1):27–39, 2005.
- P. B. Bochev, M. D. Gunzburger, and J. N. Shadid. "On inf–sup stabilized finite element methods for transient problems." Computer Methods in Applied Mechanics and Engineering 193.15-16: 1471-1489, 2004.
- E. Castillo and R. Codina. Dynamic term-by-term stabilized finite element formulation using orthogonal subgrid-scales for the incompressible Navier–Stokes problem. Computer Methods in Applied Mechanics and Engineering, 349, 701-721. 2019

UNIVERSITAT POLITÈCNICA
DE CATALUNYA
BARCELONATECH

CIMNE

CIMNE Coffe Talk

December 2019

Thank you for your attention!!

Laura Moreno Martínez